

SUBSAMPLING SPECTRAL CLUSTERING FOR LARGE-SCALE SOCIAL NETWORKS

BY JIAYI DENG¹, YI DING¹, YINGQIU ZHU¹, DANYANG HUANG^{1,*}, BINGYI JING², AND BO ZHANG^{1,†}

¹Center for Applied Statistics and School of Statistics, Renmin University of China, Beijing, China, *dyhuang@ruc.edu.cn; [†]mabzhang@ruc.edu.cn

²The Hong Kong University of Science and Technology, Hong Kong, China.

Online social network platforms such as Twitter and Sina Weibo have been extremely popular over the past 20 years. Identifying the network community of a social platform is essential to exploring and understanding the users' interests. However, the rapid development of science and technology has generated large amounts of social network data, creating great computational challenges for community detection in large-scale social networks. Here, we propose a novel subsampling spectral clustering algorithm to identify community structures in large-scale social networks with limited computing resources. More precisely, spectral clustering is conducted using only the information of a small subsample of the network nodes, resulting in a huge reduction in computational time. As a result, for large-scale datasets, the method can be realized even using a personal computer. Specifically, we introduce two different sampling techniques, namely simple random subsampling and degree corrected subsampling. The methodology is applied to the dataset collected from Sina Weibo, which is one of the largest Twitter-type social network platforms in China. Our method can very effectively identify the community structure of registered users. This community structure information can be applied to help Sina Weibo promote advertisements to target users and increase user activity.

1. Introduction. Community detection is an important research direction in social network analysis (Newman and Girvan, 2004; Fortunato, 2010), and it aims to cluster the nodes into different groups with high edge concentrations within the same cluster and low concentrations between different ones (Girvan and Newman, 2002; Lancichinetti and Fortunato, 2009). Particularly, for Sina Weibo, one of the largest Twitter-type online social network platforms in China, the registered users' community information can be applied to understand consumer market profiles. This guides the online platform to arrange suitable products, services, and resources for the target user groups and helps establish closer relationships between users. For example, as displayed in the left panel of Figure 1, each product is promoted to users according to the preferences of the user community. In this way, not only could the advertisers' chances of success be increased, but the users could also obtain satisfactory products and services (Yang et al., 2021; Shaddy and Shah, 2021; Homburg, 2021). Specifically, to increase advertisers' business opportunities, Sina Weibo shows commercial advertisements, as shown in the right panel of Figure 1, to targeted user groups. However, considering that Sina Weibo is one of the largest Twitter-type online social media in China, even if the computing techniques have improved significantly, dealing directly with such large-scale social network data remains challenging, especially when limited computing resources are available (Harenberg et al., 2014; Wang et al., 2018, 2019).

Keywords and phrases: Large-scale Social Networks, Community Detection, Subsampling, Spectral Clustering.

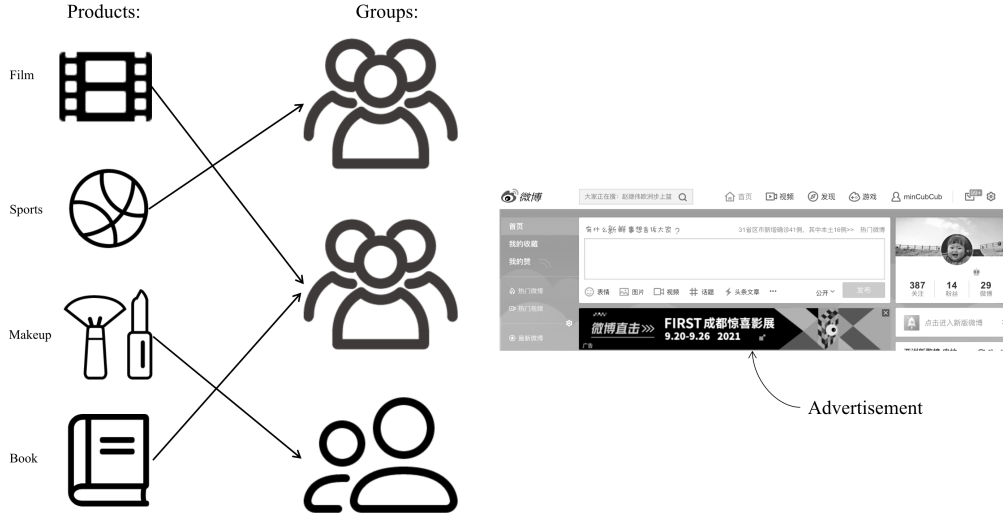


FIG 1. A product recommendation illustration is shown in the left panel, where products are delivered according to the preferences of each user group. The right panel is an example of individualized advertisement on a user's homepage.

In community detection literature, spectral clustering is one of the most popular methods because it is easy to implement and has well-founded theoretical guarantees (Ng et al., 2002; Rohe et al., 2011; Krzakala et al., 2013; Binkiewicz et al., 2017). Given a network with N nodes and K different clusters, spectral clustering embeds each node in a K -dimensional space based on singular value decomposition (SVD). The computational complexity of spectral clustering is $O(N^3)$ (Yan et al., 2009; Li et al., 2011; Chen and Cai, 2011), which is difficult to afford for large-scale social networks to afford. For example, as shown in Figure 10, conducting spectral clustering for $N = 10,000$ nodes will cost 298.446 seconds for a personal computer with a 3.70 GHz Intel Core i9 processor. For a larger $N = 30,000$, the time cost increases sharply to 6,600.103 seconds. Therefore, using spectral clustering to identify the community structures of online social network platforms presents huge computational challenges.

There has been an increasing interest in studying fast spectral clustering for large-scale social networks. Specifically, several researchers exploited the numerical solution of eigenfunction problems, the Nyström method, to speed up the eigendecomposition (Fowlkes et al., 2004; Drineas and Mahoney, 2005). Moreover, Yan et al. (2009) developed a fast approximate of spectral clustering through local data reduction, which replaces the original dataset with a small number of representative points. Chen et al. (2010) proposed the parallel spectral clustering method that first constructs a sparse similarity matrix and then calculates the embedding vector of each point in parallel. Chen and Cai (2011) proposed the landmark-based spectral clustering, which selects a few representative points as landmarks and represents the original data points as a linear combination of these landmarks. In other words, they still compute all elements of the large-scale similarity matrix. This motivates us to extend the traditional spectral clustering under the constraint of limited computing resources.

We investigate selecting a small node set to extract the network structure information with limited computational cost. Considering large-scale social networks, the network structure information is contained in the connections among nodes and can be represented by network adjacency or Laplacian matrices. However, such matrices are high-dimensional and could lead to high computational costs. To solve the problem, we propose selecting a small node

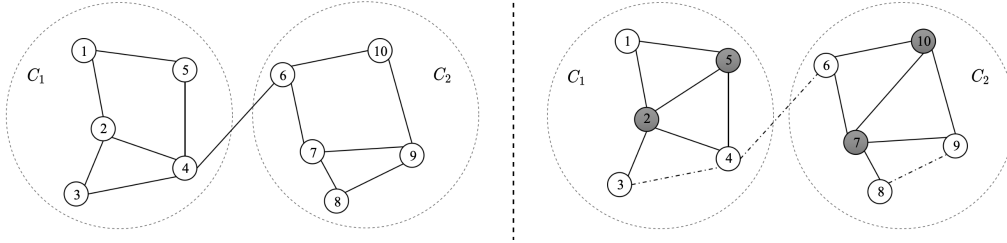


FIG 2. Example of network subsampling. A network with ten nodes and two communities (C_1, C_2) is displayed in the left panel. The right panel is a subgraph, in which the selected nodes are gray, the edges connected by selected nodes are indicated by solid lines, and the edges between unselected nodes are denoted by dashed lines.

set and then consider extracting the network community structure only through connections related to the selected nodes. To illustrate, we provide an example of network subsampling as shown in Figure 2, where the graph contains ten nodes assigned to two communities. It is remarkable that we can perfectly identify the community labels for all nodes based only on the connections related to the selected nodes. Moreover, because we only select a small subset of the total nodes, we can use a much lower dimensional matrix to represent the network nodes' connection information.

In this way, we propose a subsampling spectral clustering (SSC) method for large-scale social networks under the constraint of limited computing resources. To the best of our knowledge, this is the first study to discuss network subsampling for community detection in large-scale social networks. Specifically, we discuss two types of subsampling methods: simple random subsampling (SRS) and degree-corrected subsampling (DCS). To evaluate the efficiency of the SSC method, we apply it to a dataset with $N = 9,980$ nodes collected from Sina Weibo. As shown in Table 1, when the subsample size is 1,000 nodes, the SSC method is about 150 (298.827s/1.988 s) times faster than traditional spectral clustering, but there is little loss of accuracy. Additionally, we provide theoretical guarantees for the SSC method. Specifically, we prove that subsampling size n can be as small as $\Omega\{\log(N)\}$ based on the stochastic block model (SBM) (Holland et al., 1983). We then show that the computational complexity of the SSC method is only $O(n^2N)$. It is noteworthy that $n \ll N$, which implies that the computational complexity of the proposed method could be as low as $O(N\{\log(N)\}^2)$.

The remainder of the paper is organized as follows. In Section 2, we propose the SSC algorithm and discuss the two subsampling methods. In Section 3, we apply the SSC method to a Sina Weibo dataset and discuss the results. In Section 4, we establish the theoretical properties of the two subsampling methods. Some simulation studies are presented in Section 5. Section 6 highlights the main conclusions and discusses future research. All technical proofs are presented in the Appendices of the Supplementary Material.

2. Subsampling spectral clustering for stochastic block models. Here, we propose a spectral clustering method based on subsampling and introduce two different subsampling methods for spectral clustering in the SBM theoretical framework. The stochastic block model is an important random graph model for studying community detection (Holland et al., 1983; Rohe et al., 2011). Let $\text{Bern}(p)$ be the Bernoulli distribution with success probability $p \in [0, 1]$. Under an SBM with N nodes and K communities, define a symmetric probability matrix $B = (B_{kk'}) \in [0, 1]^{K \times K}$ and a label vector $z = (z_1, \dots, z_N)^T \in [K]^N$, where $[K] = \{1, \dots, K\}$. Then, its adjacency matrix $A = (A_{ij}) \in \{0, 1\}^{N \times N}$ is assumed to be symmetric with zero diagonals and, for all $i > j$, $A_{ij} = A_{ji} \sim \text{Bern}(B_{z_i z_j})$ independently. Specifically, in the Sina Weibo dataset, each node is a registered user, and the edge between

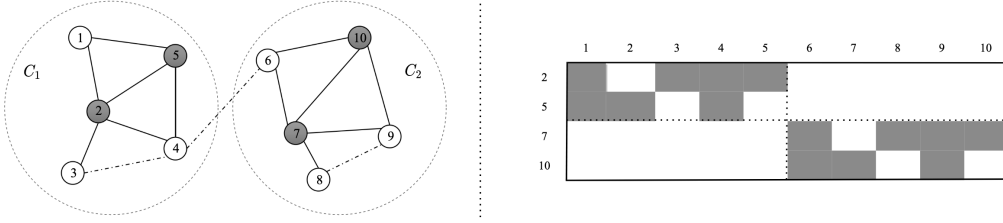


FIG 3. An illustration of a bi-adjacency matrix. The left panel displays a graph with ten nodes, two communities (C_1, C_2) and four selected nodes indicated by gray. The right panel represents the transpose of the bi-adjacency matrix, $\{A^s\}^\top$, where the gray scale indicates that there is an edge between the corresponding pair of nodes.

the node pair i, j (i.e., $A_{ij} = 1$) indicates that there is a friend relationship between users i and j . It is noteworthy that, in the SBM model, for any $i, j \in [N]$, the probability of an edge between node i and j depends only on their community memberships. Further, we define \mathcal{G} as an undirected graph generated from the SBM.

2.1. *Subsampling spectral clustering.* We propose the SSC method in a large-scale social network based on the SBM theoretical framework. Owing to computational complexity considerations, we first subsample a sub-vertex set V_s from graph \mathcal{G} and then identify network communities applying a spectral method to the subsampled Laplacian matrix.

Specifically, given network \mathcal{G} , let $V_s = \{s_j : s_j \in [N], 1 \leq j \leq n\}$, where s_j denotes the selected node. Moreover, we define a bi-adjacency matrix $A^s = (A_{ij}^s) \in \mathbb{R}^{N \times n}$, where $A_{ij}^s = A_{is_j}$ for $1 \leq i \leq N, 1 \leq j \leq n$. The bi-adjacency matrix is applied to represent the connections related to the selected node set V_s . In the SBM framework, nodes within a community often have a similar connection intensity to the selected nodes, whereas nodes in different communities have a different connection intensity from the selected nodes. For instance, we display a graph with ten nodes and two communities as shown in the left panel of Figure 3, where the selected nodes are gray. The right panel shows the transpose of bi-adjacency matrix $\{A^s\}^\top$. There are clear block structures in the bi-adjacency matrix, and nodes within a community are gathered in the same block. Therefore, based on the proper selected node set, the bi-adjacency matrix can contain almost all network community structure information. Then, we apply spectral clustering to the normalized bi-adjacency matrix. Considering that, for adjacency matrix A , its normalized Laplacian matrix can be denoted by $L = D^{-1/2}AD^{-1/2} \in \mathbb{R}^{N \times N}$, where D is a diagonal matrix with the i -th diagonal element being $\sum_j A_{ij}, (1 \leq i \leq N)$. Then, a sampled Laplacian (normalized bi-adjacency) matrix can be defined as

$$(1) \quad L^s = (D_{(r)}^s)^{-1/2} A^s (D_{(c)}^s)^{-1/2} \in \mathbb{R}^{N \times n},$$

where $D_{(r)}^s = \{\sum_j A_{ij}^s\} \in \mathbb{R}^{N \times N}$ and $D_{(c)}^s = \{\sum_i A_{ij}^s\} \in \mathbb{R}^{n \times n}$ are defined as the out- and in-degree matrices of subsampled node set V_s , respectively.

We next discuss how to obtain embedding vectors for the entire network based on the subsampled Laplacian matrix. Assume that the SVD of L^s could be expressed as $L^s = U^s \widehat{\Sigma}^s V^\top \in \mathbb{R}^{N \times n}$, where $\widehat{\Sigma}^s \in \mathbb{R}^{n \times n}$ is a diagonal matrix with the eigenvalues of L^s sorted in decreasing order. Let $U^s \in \mathbb{R}^{N \times n}$ and $V \in \mathbb{R}^{n \times n}$ denote the corresponding left and right eigenvector matrices, respectively. As a result, the SVD decomposition of $(L^s)^\top L^s \in \mathbb{R}^{n \times n}$ can be denoted as follows: $(L^s)^\top L^s = V(\widehat{\Sigma}^s)^2 V^\top = V \widehat{\Lambda} V^\top$, where $\widehat{\Lambda} = (\widehat{\Sigma}^s)^2$. Then, we have $U^s = L^s V (\widehat{\Lambda}^{1/2})^\dagger$, where M^\dagger is defined as the pseudo-inverse matrix of an arbitrary

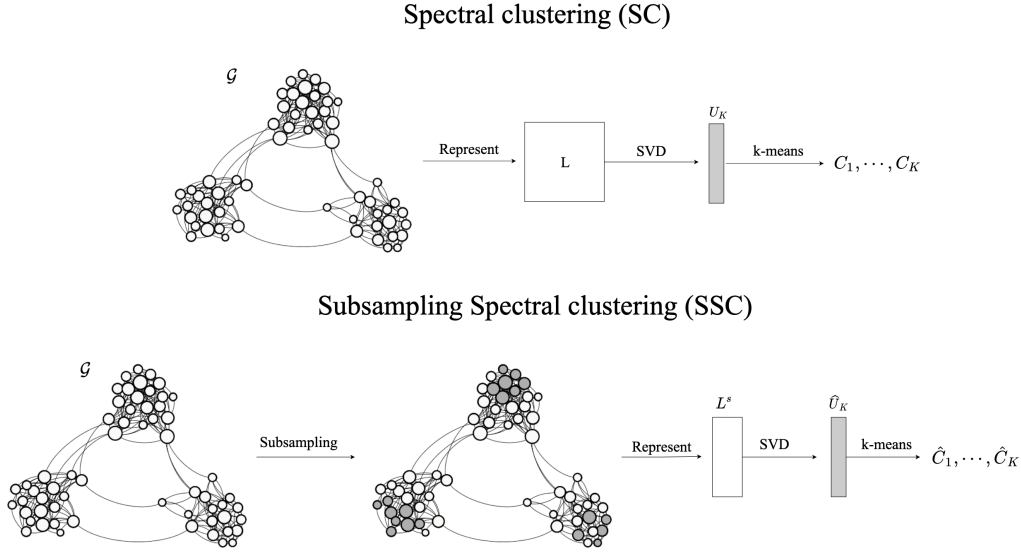


FIG 4. Comparison between spectral clustering and SSC. The upper panel represents the spectral clustering algorithm, which applies the k-means algorithm to the rows of the largest K eigenvectors of L (i.e., U_K) to obtain the clustering results. The lower panel shows the SSC algorithm, which applies subsampling to extract a subset of the entire node set where the gray nodes are the selected ones. Then, we form a subsampled Laplacian matrix L^s , and, through spectral analysis, we find its largest K left eigenvectors, \hat{U}_K . We also apply the k-means algorithm to the rows of \hat{U}_K to obtain the clustering results.

matrix, M . Furthermore, let $\hat{U}_K \in \mathbb{R}^{N \times K}$ be the matrix containing left K eigenvectors of L^s corresponding to its largest K eigenvalues. Then,

$$(2) \quad \hat{U}_K = L^s V_K (\hat{\Lambda}_K^{1/2})^\dagger,$$

where $\hat{\Lambda}_K^{1/2} \in \mathbb{R}^{K \times K}$ is defined as a diagonal matrix with K largest eigenvalues of $(L^s)^\top L^s$, and V_K being a matrix that contains the right K eigenvectors of $(L^s)^\top L^s$ corresponding to its largest K eigenvalues. We consider \hat{U}_K as the approximated embedding vectors of all network nodes. Then, community membership can be obtained by applying the k-means algorithm to the rows of \hat{U}_K . Additionally, the partition results are recorded by $\hat{C}_k = \{i : \hat{z}_i = k, 1 \leq i \leq N\}$ ($k = 1, \dots, K$), where \hat{z}_i is the estimated label of node i . For simplicity, the extension of a spectral clustering algorithm by subsampling is referred to as the SSC method. The following proposition describes the computational complexity of this method.

PROPOSITION 2.1 (Computational complexity). *For a graph \mathcal{G} with N nodes, assume that n nodes are subsampled from \mathcal{G} . Then, the computational complexity of community detection for the entire graph, \mathcal{G} , based on the SSC algorithm is $O(n^2 N)$.*

The proof of Proposition 2.1 is provided in Appendix B.1 of the Supplementary Material. The SSC's computational complexity is significantly lower than that of the traditional spectral clustering method based on the entire network. Proposition 2.1 shows that, for limited computing resources, the SSC algorithm could be applied to reduce the computational burden of community detection for large-scale social networks.

To further illustrate the proposed method, we compare SSC with the traditional spectral clustering algorithm for the entire network in Figure 4. Evidently, unlike the traditional spec-

Algorithm 1 Subsampling spectral clustering (SSC)

Input: Graph \mathcal{G} , adjacency matrix $A \in \mathbb{R}^{N \times N}$, subsample node set $V_s = \{s_j : s_j \in [N], 1 \leq j \leq n\}$, number of communities K ;

1. Form bi-adjacency matrix $A^s \in \mathbb{R}^{N \times n}$ and compute its subsampled Laplacian matrix, $L^s \in \mathbb{R}^{N \times n}$, as defined in (1);
2. Conduct SVD on $(L^s)^\top L^s$ and find its largest K eigenvalues and the corresponding eigenvectors;
3. Compute the approximation embedding vectors, \hat{U}_K , as defined in (2);
4. Conduct k-means to cluster the rows of \hat{U}_K into K clusters $\hat{C}_1, \dots, \hat{C}_K$.

Output: Partition results $\hat{C}_1, \dots, \hat{C}_K$.

tral clustering method, SSC creates a subsampled Laplacian matrix with a much lower column dimension based on the small subsample. In other words, SSC is conducted on a small part of the connections in the entire network. Consequently, its clustering results may not be as accurate as those obtained by spectral clustering. However, it can obtain cluster labels for the entire network with limited computing resources. This could make network clustering feasible even using a personal computer.

The SSC procedure is described in Algorithm 1 and has several advantages. First, it overcomes the challenges of handling large-scale social networks with limited computing resources. We only focus on selected nodes that are generated by subsampling and can identify the community structure using the connection information between the selected and entire node sets. Second, it is more flexible than classical spectral clustering because we can control subsample size n to balance accuracy and computational cost. Third, the SSC method is highly efficient. With a small subsample size, SSC can almost perfectly identify the community labels for all network nodes. This will be demonstrated in detail in the next few sections.

REMARK 2.2 (Choosing the number of clusters). Here, we discuss how to choose the number of clusters, K . Inspired by [Von Luxburg \(2007\)](#), the eigengap heuristic can be adopted in the SSC algorithm. Let $\hat{\lambda}_1 \geq \hat{\lambda}_2 \geq \dots \hat{\lambda}_n$ denote eigenvalues of the subsampled Laplacian matrix. The eigengap heuristic aims to identify the value of K satisfying that all $\hat{\lambda}_1, \dots, \hat{\lambda}_K$ are large enough, but $\hat{\lambda}_{K+1}$ is small. Specifically, an appropriate number of clusters can be obtained by the following three steps. First, we compute the eigenvalues of L^s and sort them in descending order. Second, we generate sequence $W = (w_1, \dots, w_{n-1})^\top \in \mathbb{R}^{n-1}$, where $w_k = \hat{\lambda}_k - \hat{\lambda}_{k+1}$ for $k = 1, 2, \dots, n-1$. Finally, we select K satisfying $K = \operatorname{argmax}_k w_k$ as the appropriate number of clusters.

Intuitively, the subsampling method could affect the performance of the SSC. Next, we discuss two different subsampling methods and their corresponding theoretical properties.

2.2. Two subsampling methods. Here, we introduce two subsampling methods for spectral clustering under the SBM theoretical framework. In SBM, the link probabilities between node pairs depend only on their communities. Then, in terms of network structure information, the nodes in the same community have equal importance. Further, there are apparent differences in connection strength within and between communities. We first discuss SRS, and then, based on the stochastic block model, we design the DCS.

Simple random sampling is a uniform subsampling method, where the subsampling distribution is $p_i = n/N$ for $i = 1, 2, \dots, N$. We choose the nodes accordingly to obtain a subsampled node set V_s from \mathcal{G} in the first step. Then, using SSC, the network clustering results can be obtained as desired. For simplicity, we refer to this procedure as SRS-SC. According

to [Vitter \(1985\)](#), the computational complexity of subsampling by SRS is $O(N)$. Therefore, by [Proposition 2.1](#), the computational complexity of SRS-SC is also $O(n^2N)$.

As previously discussed, our proposed method depends on selected node set V_s . Ideally, an informative subsample should have the following two properties. First, node set V_s contains nodes from K different blocks. Second, the nodes in V_s have dense connections with the unselected nodes to ensure that the set contains more network structure information. However, we cannot always generate a subsample like this by using SRS. This motivates us to design a degree-corrected subsampling spectral clustering algorithm.

Considering the properties of the SBM, all nodes within the same community have the same degree distribution. Therefore, the degrees of the nodes provide important network structure information. For robustness, we regularize the node degree sequence. That is, we define a regularized degree sequence as $\hat{f}_i = \hat{d}_i/N$, where $\hat{d}_i = \sum_j A_{ij}$ is the observed degree of the i -th node, for $i = 1, 2, \dots, N$. Then, for an observed network, we have an initial node set partition applying the k-means algorithm to the regularized degree sequence. We denote this initial partition as C_1^0, \dots, C_K^0 , where C_k^0 is the node set of the k -th cluster and $\bigcup_{k=1}^K C_k^0 = [N]$. Next, we sample the node set from C_1^0, \dots, C_K^0 . To collect more network connection information, for $k = 1, \dots, K$, we sort the nodes in the k -th cluster C_k^0 according to their regularized degrees in decreasing order. Then, we take the first $n|C_k^0|/N$ nodes from sorted node set C_k^0 , where $|C_k^0|$ is the size of C_k^0 . Therefore, these selected nodes have more connections with the unselected nodes than the randomly selected nodes from this set. We refer to it as DCS.

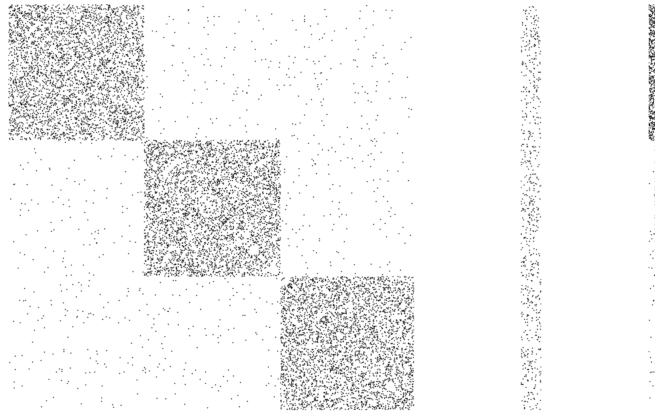


FIG 5. *The plot of the adjacency matrix (left panel), bi-adjacency matrix formed by SRS (middle panel), and bi-adjacency matrix formed by DCS (right panel).*

To illustrate the intuition of the DCS method, we generate a network from SBM with 6,000 nodes and three communities and set the subsample size to $n = 300$. Here, the community labels of the nodes are generated from an independent multinomial distribution with $\pi = (1/3, 1/3, 1/3)^\top$. For comparison, we plot the original adjacency and the bi-adjacency matrices formed by SRS and DCS, respectively. In these matrices, white indicates zero elements and black, nonzero elements. Furthermore, the rows and columns have been rearranged according to the community structure. Evidently, as seen in the adjacency matrix (left panel), there are three blocks that represent three communities in this network. However, as seen in the middle panel of [Figure 5](#), the community structure is not easy to identify based on the bi-adjacency matrix formed by SRS. Although the subsample node set covers three communities, the differences in the intensity connections within and between the communities are

unclear. In contrast to SRS, there are clear boundaries for each block of the bi-adjacency matrix formed by DCS. Because the connection intensity within blocks is significantly larger than that between blocks, the bi-adjacency matrix formed by DCS is more useful in identifying network communities. We prove this conclusion theoretically in the next section.

As previously discussed, the DCS method obtains the subsampled node set in two steps. The first step derives an initial partition using node degree information. It is a tentative description of node heterogeneity. The second step is a refinement procedure, which helps extract relatively influential nodes in each cluster. In this way, the subsampled node set has clearer boundaries between community blocks. Furthermore, compared with SRS, DCS selects subsampled nodes that have more connections with the unselected ones. The DCS algorithm is presented in Algorithm 2.

Algorithm 2 Degree-corrected subsampling (DCS) method

Input: Graph \mathcal{G} , adjacency matrix $A \in \mathbb{R}^{N \times N}$, sample size n , number of communities K ;

1. Compute regularized degree sequence $\hat{f}_i = 1/N \sum_j A_{ij}$, for $i = 1, \dots, N$;
2. Perform k-means clustering to the regularized degree sequence to obtain the initial nodes partition, C_1^0, \dots, C_K^0 ;
3. Sort each cluster's node decreasingly according to the node degree;
4. Form the subsampled node set V_s by choosing the first $n|C_k^0|/N$ nodes from node set C_k^0 for $k = 1, 2, \dots, K$.

Output: Subsampled node set V_s .

In general, DCS outputs a subsampled node set, V_s . Then, the partition results for the whole network can be obtained by SSC. For simplicity, this procedure is referred to as DCS-SC.

3. A Sina Weibo dataset. We apply the SSC algorithm to a dataset collected from Sina Weibo (*www.weibo.com*). Similar to Twitter, Sina Weibo allows different users to follow each other, which leads to a large-scale social network. For this example, we start with the official Weibo account of a Master of Business Administration (MBA) program in China. Because of a constraint imposed by Sina Weibo's application programming interface (API) and after omission of isolated nodes, we collect a social network with $N = 9,980$ users. Ideally, we would like to analyze the social network structure of the collected users using our proposed methods.

3.1. Data illustration. An undirected network is constructed based on this dataset. Each node is a user, and an edge exists if there is a friend relationship between two users. Given any two users, i and j , the corresponding element of the adjacency matrix A_{ij} is set to 1 if there is at least one edge between two users. This leads to 1,325,604 undirected edges. The density of the social network is $\sum_{ij} A_{ij} / \{N(N-1)\} = 0.027$. In the following, we study the Sina Weibo dataset further.

As shown in the top panel of Figure 6, we display the histogram of the degree sequence of this social network. Evidently, this degree distribution is highly right-skewed, and a small percentage of these nodes have much more connections than most other nodes. In other words, some users have gained a lot of attention and high influence in Sina Weibo. To demonstrate the degree distribution of subsampling in extracting social network information, we sample $n = 200$ nodes from the entire collected social network by using SRS and DCS. Consequently, we obtain a bi-adjacency matrix $A^s \in \mathbb{R}^{N \times n}$ and its out-degree sequence $\{D_{(r)}^s\}_{ii} = \sum_j A_{ij}^s$, for $i = 1, \dots, N$. For comparison, in the bottom panel of Figure 6, we

plot the distribution of the out-degree sequence. Noteworthy, both out-degree distributions capture the characteristic of right-skewness, and the out-degree distribution based on DCS has a heavier tail than that based on SRS as DCS tends to select nodes with a larger degree.

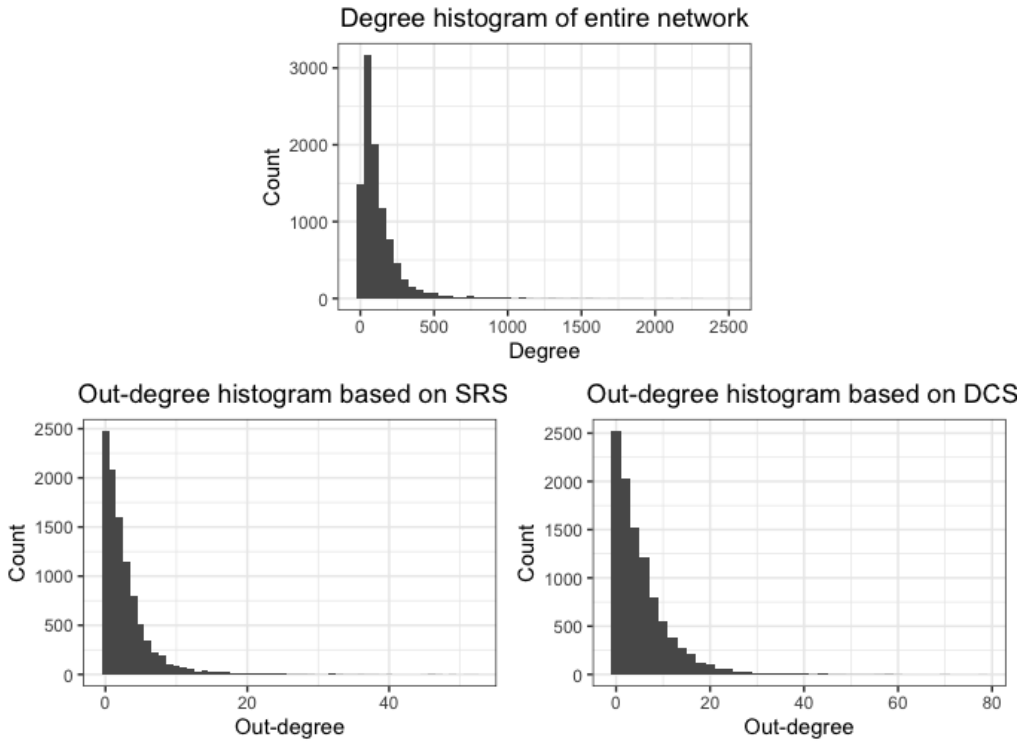


FIG 6. The histogram of the Sina Weibo social network, with degree distribution that is heavily right-skewed. The top panel is the degree histogram of the entire collected Sina Weibo network. The bottom left and right panels show the out-degree distributions of the subgraphs extracted by SRS and DCS, respectively.

Identification of network communities is an important tool in market segmentation analysis in marketing. Network community detection approaches could be applied to understand the consumer market profile. For online social network platforms, various marketing strategies could be applied to different users to make them more active on the platform. Additionally, an efficient recommendation system can be established to promote products to target communities, thereby bringing more business opportunities to advertisers. In this study, to further illustrate the heterogeneity in the network, we select three representative nodes: “singer”, “gourmet”, and “programmer”. Their connected nodes are also collected. Accordingly, we plot a subnetwork of the collected social network. Figure 7 shows that the connections within some nodes (e.g., connections within neighbors of the “programmer”, where “neighbors” means connected nodes) are denser than those among others (e.g., connections between neighbors of the “singer” and the “programmer”). This means that nodes may form different groups. Therefore, for a better understanding of users’ profiles, we aim to cluster them into different groups. In this way, diversified marketing strategies could be developed. Figure 7 presents an example of the application of the clustering results, wherein a computer advertisement would be better presented to the nodes connected to “programmer” rather than those connected to “gourmet.” To analyze the community information contained in the social network further, we need to conduct community detection and analysis.

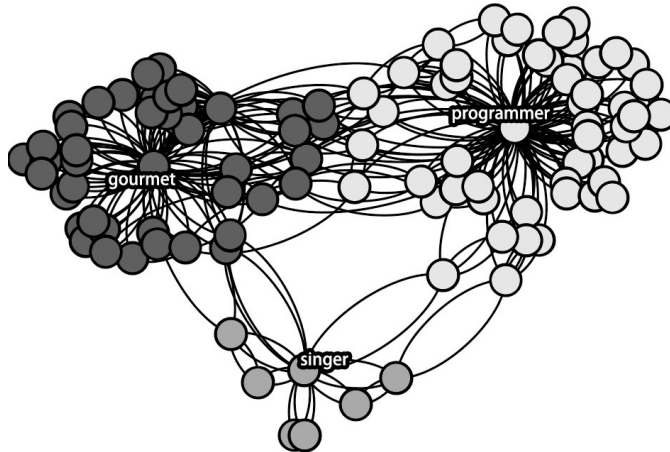


FIG 7. The plot of the subnetwork composed of three centroid nodes (i.e., “singer”, “gourmet”, and “programmer”) and their neighborhood nodes. These centroid nodes are marked with the occupation of the corresponding users, and the colors of the neighborhood nodes are identical to those of the corresponding centroid nodes.

3.2. *Community structure of the entire collected social network.* In this section, we investigate the community structure of the entire collected social network. Because the true community labels are unknown in the real data analysis, we discuss the partition performance by spectral clustering using the entire collected social network.

Specifically, according to the eigengap method discussed in Remark 2.2, the number of communities is selected as $K = 3$. In Figure 8, we display two eigenvectors corresponding to the first and second largest eigenvalues of the Laplacian matrix. The type of scatter point indicates the community membership of the corresponding node. Obviously, the embedding vectors of network nodes have a clear community structure. This indicates that spectral clustering is feasible for identifying the community membership of this social network. As a result, we obtain clustering results with three communities, whose sizes are 5,429, 4,119, and 432. However, the computational time is 298.827 seconds on a Dell computer with a 3.70 GHz Intel Core i9 processor. This could lead to infeasibility in real large-scale social network data. Next, we take the cluster labels derived by spectral clustering as ground truth to evaluate the proposed methods, that is, SRS-SC and DCS-SC.

3.3. *Application of the SRS-SC and DCS-SC algorithms.* Here, we evaluate the ability of our method to identify the community structure of a large-scale social network and reduce the computational complexity in the application. In the first step, we compare the clustering results between the proposed methods and the spectral clustering results obtained from subsection 3.2. Then, we further study the common interests within each community obtained by the proposed method. Last, we provide some examples to illustrate the applications of community structure information.

Considering that the true community labels are unknown, the misclustered rate is defined here to measure the dissimilarity of community assignments between the spectral clustering results and the SSC algorithm results. Specifically, let $\tilde{Z} \in \mathbb{R}^{N \times K}$ denote the community membership matrix obtained by spectral clustering. Accordingly, let $\hat{Z} \in \mathbb{R}^{N \times K}$ denote the estimated membership matrix obtained by SSC. Then, the misclustered rate is calculated by $\mathcal{R}(\hat{Z}, \tilde{Z}) = N^{-1} \min_{\theta \in \mathbb{E}_K} d(\hat{Z}\theta, \tilde{Z})$ defined as in (7). Table 1 shows the misclustered rate,

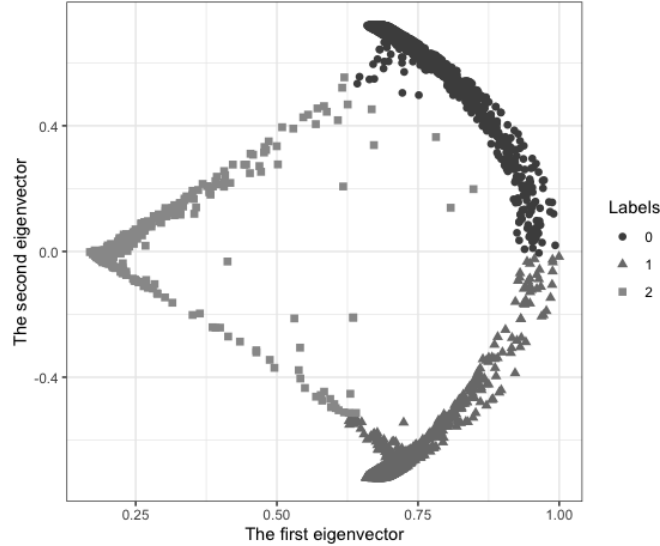


FIG 8. The largest two eigenvectors corresponding to the network Laplacian matrix. The x-axis provides the largest eigenvector and the y-axis the second largest eigenvector values. The type of scattered points represents the community label.

TABLE 1

Performance of SRS-SC and DCS-SC with n varying from 200 to 1,000. The misclustered rate (MisRate) and average computation time (CPU) of SRS-SC and DCS-SC are reported accordingly. In addition, the standard error of the misclustered rate is reported in parentheses.

| | n | 200 | 400 | 600 | 800 | 1000 |
|--------|---------|------------|------------|------------|------------|------------|
| SRS-SC | MisRate | .179(.003) | .106(.001) | .075(.001) | .056(.001) | .043(.000) |
| | CPU | .404 | .668 | .957 | 1.232 | 1.785 |
| DCS-SC | MisRate | .118(.000) | .065(.000) | .044(.000) | .034(.000) | .028(.000) |
| | CPU | .674 | .958 | 1.217 | 1.485 | 1.988 |

average computational time, and standard error of the clustering results of the SSC algorithms with 100 repetitions.

We can draw the following conclusions from Table 1. First, as the subsample size n increases from 200 to 1,000, the misclustered rate of both methods drops. In particular, when $n = 200$, the DCS-SC misclustered rate is 0.118, that is, the community label obtained by DCS-SC is 88.2% identical to the label obtained in spectral clustering using the entire collected social network. Second, as n increases from 200 to 1,000, the average computational time of our proposed methods is no more than 1.988 seconds, which shows that our proposed method leads to a significant improvement in calculation. For even larger social networks, the SSC method is feasible, even using a personal computer, for obtaining cluster labels for the entire collected social network. Third, DCS-SC is more stable and has higher clustering accuracy than SRS-SC. This corroborates the conclusions we obtained in Theorem 4.7.

To understand the characteristics of each cluster, we analyze the text information posted by the users of this social network. The community partition is obtained by the DCS-SC method and the subsample size $n = 200$. As shown in Figure 9, we plot three *word clouds* to depict the representative keywords of each community. The keywords of each community are generated by gathering the Sina Weibo content posted by users. The sizes of the keywords reflect word frequency, and the shapes of word clouds are related to high-frequency words. There are clear differences between the word clouds. Based on these word clouds, members of different

communities have distinct interests and play different roles in the social network. Users assigned to the first cluster are highly concerned about news, as the high-frequency keywords in their blogs are “TV station” and “news”. The second cluster includes users who are interested in fashion and art, and their high frequency keywords are “design”, “Brand”, and “works”. The third cluster is a group with a wide range of hobbies, and it has high-frequency keywords such as “League”, “film”, and “coffee”. As an application of the community detection results, fashion products with high level of creativity meet the preferences of users in the second cluster. Besides, the services and products of tourism industries can be promoted to customers in the third cluster. Moreover, tourism services and products can be promoted to customers in the third cluster. A more detailed analysis could be conducted on different clusters to support more diversified business decisions.



FIG 9. *The word clouds of the social network communities discovered by DCS-SC. The shapes of word clouds represent the community label and the sizes of the words, their frequencies. The left panel includes representative words related to news. The middle panel implies that the users are engaged in work related to fashion and art. The right panel shows that the users in this community are used to sharing their leisure habits.*

4. Theoretical properties of the SSC algorithms. In this section, we first discuss the clustering accuracy of the SRS-SC algorithm in three steps. First, we establish the theoretical properties of the SRS-SC algorithm based on population analysis. Second, we show the consistency of eigenvectors. Third, we provide the upper bound of the misclustered rate caused by the SRS-SC algorithm. Similarly, we could establish the theoretical properties of DCS-SC.

4.1. *Population analysis of the SRS-SC algorithm.* For an observed social network, we know that the SRS-SC algorithm is applied to the adjacency matrix. Population analysis implies that we discuss the theoretical properties of SRS-SC based on the SBM probability matrix defined as (3), rather than the adjacency matrix. Following the theoretical analysis technique of Joseph et al. (2016), we establish the properties of the SRS-SC algorithm based on population analysis. As a result, we establish that the embedding vectors obtained by the observed subsampled Laplacian matrix converge to those derived by the population subsampled Laplacian matrix. Then, the upper bound of the misclustered rate for the SRS-SC algorithm based on subsampled network data can be established as desired.

We introduce more network notations corresponding to the population subsampled Laplacian matrix as follows. We denote the SBM probability matrix (population adjacency matrix) as

$$(3) \quad \mathcal{A} = ZBZ^T \in \mathbb{R}^{N \times N},$$

where $Z \in \{0, 1\}^{N \times K}$ is a membership matrix, with each row having only one nonzero entry, $Z_{iz_i} = 1$. Then, the population Laplacian matrix is $\mathcal{L} = \mathcal{D}^{-1/2} \mathcal{A} \mathcal{D}^{-1/2}$, where \mathcal{D} is the degree matrix of \mathcal{A} . Similarly, under the SSC algorithm, the population bi-adjacency matrix is defined as $\mathcal{A}^s \in \mathcal{R}^{N \times n}$ and the corresponding subsampled Laplacian matrix as $\mathcal{L}^s = (\mathcal{D}_{(r)}^s)^{-1/2} \mathcal{A}^s (\mathcal{D}_{(c)}^s)^{-1/2} \in \mathbb{R}^{N \times n}$. Furthermore, the approximation embedding vectors are the largest K left eigenvectors of \mathcal{L}^s , denoted by \widehat{U}_K .

Then, we discuss the minimum sample size, n , required for subsampling. The estimation of the network community labels relies on the connection information between the entire node set and the selected nodes. For accuracy, the selected node set should contain nodes from all communities in the entire node set. Then, the desired situation is that the selected node set V_s already contains nodes from K different blocks. Assume the block sizes of the entire network are N_1, \dots, N_K , respectively, satisfying $\sum_{k=1}^K N_k = N$. Correspondingly, let n_k denote the size of subsampled vertex set V_s belonging to the k -th block for $k = 1, 2, \dots, K$. Therefore, a desired event can be defined as $e = \{n_k : 1 \leq k \leq K, n_k \in \mathbb{Z}^+, \sum_k n_k = n\}$, where \mathbb{Z}^+ is the set of all positive integers.

Next, based on the population analysis, we provide the lower bound of the necessary sample size, n , to ensure event e is happening with high probability. We define $N_{\min} = \min\{N_1, \dots, N_K\}$, and $\alpha = N_{\min}/N$. Under SBM with K blocks, assume the sample nodes are collected through simple random sampling with replacement. Then, we have the following proposition.

PROPOSITION 4.1 (Required subsample size). *For any $\epsilon > 0$, if the subsample size is*

$$n \geq \frac{\log(K/\epsilon)}{\log\{1/(1-\alpha)\}},$$

event e happens with a probability of at least $1 - \epsilon$.

The proof of Proposition 4.1 is provided in Appendix B.2 of the Supplementary Material. Proposition 4.1 gives the lower bound of the subsampling size to ensure the subsampled node set V_s contains K blocks with high probability. It is noteworthy that the lower bound of subsample size n depends on two factors: (1) the number of blocks K and (2) the imbalance level of block size α . Specifically, if the network contains many blocks, subsample size n should be relatively large. Additionally, the imbalance level is negatively correlated with subsample size n . In this study, we consider imbalance level $\alpha = \Omega\{1/\log(N)\}$, where $\Omega\{g(N)\}$ means that, for the set of all $f(N)$, there exist positive constants a_0 and N_0 such that $f(N) \geq a_0 g(N)$ for all $N \geq N_0$ (Knuth, 1976). In this case, the required minimum sample size is $n = \Omega\{\log(1/\epsilon) \log(N)\}$. Ideally, if the nodes are uniformly distributed among different communities, the minimum required sample size is only $\Omega\{\log(1/\epsilon)\}$. This implies that, for a social network with limited blocks and uniform block size, the required sample size n can be quite small.

Next, we discuss the block structure of population approximation embedding vectors \widehat{U}_K obtained by using the SRS-SC method. The following proposition shows the connection between the membership matrix Z and population approximation embedding vectors \widehat{U}_K .

PROPOSITION 4.2 (Structure of eigenvectors). *Assume that subsampled vertex set V_s is generated by SRS. If the sample size is $n \geq \log(K/\epsilon)/[\log\{1/(1-\alpha)\}]$, for any $\epsilon > 0$, there exists a matrix $\mu \in \mathbb{R}^{K \times K}$ such that $\widehat{U}_K = Z\mu$. Furthermore,*

$$Z_i \mu = Z_j \mu \iff Z_i = Z_j,$$

with a probability of at least $1 - \epsilon$, where $Z \in \mathbb{R}^{N \times K}$ is a membership matrix, and Z_i is the i -th row of Z .

The proof of Proposition 4.2 is provided in Appendix B.3 of the Supplementary Material. From Proposition 4.2, the population approximation embedding vectors have exactly K distinct rows. More importantly, if the i -th and j -th rows of \widehat{U}_K are equal (i.e., $Z_{i\mu} = Z_{j\mu}$), nodes i and j belong to the same cluster. This is an important conclusion for the SSC algorithm. Recall that, in the SSC algorithm, k-means clustering is applied to the rows of observed embedding vectors \widehat{U}_K . Then, under the mild conditions discussed in the next section, one can verify that \widehat{U}_K converges to \widehat{U}_K . Therefore, \widehat{U}_K has roughly K distinct rows as well. Applying k-means clustering to \widehat{U}_K , we can estimate the block membership matrix Z . Next, we establish the theoretical properties of SRS-SC empirically.

4.2. *Upper bound of the misclustered rate based on the SRS-SC algorithm.* As previously discussed, we have shown that the population embedding vectors obtained by the SRS-SC algorithm have exactly K distinct rows. Next, we show the consistency of the largest K left eigenvectors of the empirical subsampled Laplacian matrix. Consequently, the upper bound of the misclustered rate caused by the SRS-SC algorithm can be established.

Before establishing the properties of SRS-SC at an empirical level, we make the following assumptions.

- (A1) (Imbalance level) Assume the cluster size imbalance level $\alpha = \Omega\{1/\log(N)\}$;
- (A2) (Required subsample size) Assume the subsampled size $n = \Omega(\{\log(N)\}^2)$;
- (A3) (Network sparsity) Assume that the minimum degree is $\delta_n = \min_i\{(\mathcal{D}_{(r)}^s)_{ii}\} \geq b_0 n$, where $0 < b_0 < 1$ is a constant.

Assumption (A1) is introduced to specify the cluster size imbalance level, as also discussed by Lei et al. (2015). That is, we allow the sample sizes in different clusters to be of different orders to some extent. Assumption (A2) ensures that the requirement of Proposition 4.1 is satisfied. For simplicity, we take $\epsilon = N^{-1/2}$. Typically, in a large-scale dataset, N is extremely large so that ϵ could be small enough. Assumption (A3) is a necessary condition to ensure the connection intensity between the entire node set and the subsampled node set. Let $b_0 = \min_{1 \leq k, k' \leq K} B_{kk'}$. One can verify that $\delta_n = \min_i\{(\mathcal{D}_{(r)}^s)_{ii}\} = \min_i\{\sum_{j=1}^n B_{z_i z_{s_j}}\} \geq n b_0$. Consequently, δ_n can grow almost linearly with n as b_0 being a constant and $0 < b_0 < 1$. Based on these assumptions, we illustrate the convergence of eigenvectors in the next theorem.

THEOREM 4.3 (Convergence of eigenvectors). *Assume $\lambda_1 \geq \dots \geq \lambda_K$ are the eigenvalues of subsampled Laplacian matrix \mathcal{L}^s . If Assumptions (A1)–(A3) are satisfied, there exists an orthogonal matrix $\mathcal{O} \in \mathbb{R}^{K \times K}$ such that*

$$(4) \quad \|\widehat{U}_K - \widehat{U}_K \mathcal{O}\|_F \leq \frac{6\sqrt{6}}{\lambda_K} \sqrt{\frac{K \log\{4\sqrt{N}(N+n)\}}{\delta_n}}$$

with a probability of at least $(1 - N^{-1/2})^2$.

The proof of Theorem 4.3 can be found in Appendix B.5 of the Supplementary Material. To illustrate the estimation error bound given in (4), we provide the following explanations. First, the error bound is related to λ_K . According to Rohe et al. (2011), λ_K is the eigengap of \mathcal{L}^s . Moreover, they pointed out that the eigengap cannot be too small. An adequate eigengap ensures that the population embedding vectors can be estimated well. Second, the error bound is lower if minimum degree δ_n is higher. To reduce the upper bound of the distance between \widehat{U}_K and \widehat{U}_K , the subgraph generated by SRS cannot be too sparse. Thus, if λ_K can be lower bounded by a positive constant and $\delta_n \gg K \log(N)$, then we have $\|\widehat{U}_K - \widehat{U}_K \mathcal{O}\|_F = o_p(1)$.

Third, the upper bound is also related to the number of clusters, K , and the subsample size, n . Recall that Proposition 4.1 implies that the subsample size n depends mainly on the imbalance level α . Therefore, if the number of clusters, K , and the imbalance level, α , are relatively large, it is difficult to identify the network communities. This conclusion is identical to that of Lei et al. (2015).

Next, we focus on the clustering error of SRS-SC. First, we give a sufficient condition for a node to be clustered correctly. Subsequently, according to this condition, we define a misclustered set. Finally, we establish the upper bound of the size of the misclustered set in Theorem 4.5.

Let $c_i \in \mathbb{R}^K$ denote the centroid of the cluster, to which the i -th row of \widehat{U}_K belongs, for $i = 1, 2, \dots, N$. Based on Proposition 4.2, $Z_i\mu$ is the centroid corresponding to the i -th row of \widehat{U}_K . Hence, if the observed centroid c_i is closer to the population centroid $Z_i\mu$ than any other population centroid $Z_j\mu$ for all j with $j \neq i$, node i is considered correctly clustered. Specifically, we provide a sufficient condition for a node to be clustered correctly as follows.

PROPOSITION 4.4 (Clustered correctly). *Node i is clustered correctly if*

$$\|c_i - Z_i\mu\mathcal{O}\| \leq \frac{1}{\sqrt{2N_{\max}}},$$

where $N_{\max} = \max\{N_1, \dots, N_K\}$ is the size of the largest block.

The proof of the Proposition 4.4 is provided in Appendix B.4 of the Supplementary Material. Based on Proposition 4.4, we can define the misclustered node set as $\mathcal{R} = \{i : \|c_i - Z_i\mu\mathcal{O}\| > (2N_{\max})^{-1/2}\}$. Based on this definition, we then provide the upper bound of misclustered rate $|\mathcal{R}|/N$.

THEOREM 4.5 (Upper bound of the misclustered rate). *Assume that Assumptions (A1)-(A3) are satisfied. Then, there exists a constant c_0 such that*

$$(5) \quad \frac{|\mathcal{R}|}{N} \leq \frac{c_0 N_{\max} K \log\{4\sqrt{N}(N+n)\}}{Nn\lambda_K^2},$$

with a probability of at least $(1 - N^{-1/2})^2$.

The proof is provided in Appendix B.6 of the Supplementary Material. Based on Theorem 4.5, we can draw the following conclusions. First, by (5), the misclustered rate decreases as the subsample size n increases. Second, in the special case of balanced community sizes (i.e., $KN_{\max} = O(N)$) and positive constant K and λ_K , if $n \geq \{\log(N)\}^2$, then $|\mathcal{R}|/N = O\{\log(N)^{-1}\}$.

4.3. *Theoretical analysis of the DCS-SC algorithm.* For simplicity, we introduce some necessary notations as follows: recall that the observed regularized degree sequence is $\hat{f}_i = N^{-1} \sum_j A_{ij}$, $i = 1, 2, \dots, N$. Under the SBM, these are independent random variables with expectation $f_i = E(\hat{f}_i)$ for $i = 1, 2, \dots, N$. The matrix expression can be denoted by $\widehat{F} = (\hat{f}_1, \dots, \hat{f}_N)^\top$, $F = (f_1, \dots, f_N)^\top \in \mathbb{R}^N$. Consider that the DCS algorithm applies k-means clustering to the regularized degree sequence, $\hat{f}_1, \dots, \hat{f}_N$, in the first step. Let \widehat{F}_k denote the centroid of the k -th cluster for $k = 1, 2, \dots, K$. Further, define $\Delta_k = N_k^{-1/2} \|\widehat{F}_k - F\| = \sqrt{\sum_i (\hat{f}_i - f_i)^2 / N_k}$. Then, the detailed assumptions are as follows:

- (A1) (Degree blocks) Assume that the expectation of regularized degree sequence F contains exactly K distinct elements. Moreover, for $k = 1, 2, \dots, K$ and $i = 1, 2, \dots, N$, if $z_i = k$, let $F_k = f_i$;
- (A2) (Separation condition) Assume that, for any $1 \leq k, k' \leq K$, $k \neq k'$, $|F_k - F_{k'}| \geq c(N_k^{-1/2} + N_{k'}^{-1/2})\|\widehat{F} - F\|$, where c is a large constant.

Assumption (A1) is introduced to ensure that the degree sequence can be partitioned into distinct K blocks. Further, assume the stochastic block model is defined as in (6). Then, the elements of F can be expressed as $f_i = (N - N_{z_i})\beta\zeta + (N_{z_i} - 1)\beta = \beta\{(N\zeta - 1) + N_{z_i}(1 - \zeta)\}$, for $i = 1, 2, \dots, N$. Therefore, under this condition, if block sizes N_1, \dots, N_K are different, Assumption (A1) can be satisfied. Assumption (A2) is widely used to ensure good performance of the k-means clustering algorithm (Awasthi and Sheffet, 2012). Under the above assumptions, we posit the following proposition on the required subsample size of DCS-SC.

PROPOSITION 4.6 (Required subsample size). *Under an SBM with K blocks, assume the sample nodes are obtained by the DCS algorithm. For any $\epsilon > 0$, if Assumptions (A1)-(A2) are satisfied and the subsample size is $n \geq 64 \log(2N\epsilon^{-1})$, event e happens with a probability of at least $1 - \epsilon$.*

The proof of Proposition 4.6 can be found in Appendix C.1 of the Supplementary Material. Proposition 4.6 implies that, by the DCS algorithm, if the subsample size is $n = \Omega\{\log(N)\}$, the subsample node set can contain nodes from all network blocks with high probability. Intuitively, the DCS algorithm collects network structure information more effectively than that of SRS. Next, we establish the upper bound of the misclustered rate caused by the DCS-SC algorithm.

THEOREM 4.7 (Misclustered rate). *From Assumptions (A1)-(A2), if subsample size $n \geq 24 \log(2N)$ and the minimum expected average degree $\delta_n = \min_i\{(D_{(r)}^s)_{ii}\}$ satisfy Assumption (A3), there exists a constant c_1 such that*

$$\frac{|\mathcal{R}|}{N} \leq \frac{c_1 N_{\max} K \log\{4\sqrt{N}(N+n)\}}{N n \lambda_K^2},$$

with a probability of at least $(1 - N^{-1/2})^2$.

As the proof of Theorem 4.7 is similar to that of Theorem 4.5, we omit a detailed proof here. Based on Theorem 4.7, the required subsample size for DCS-SC is $n \geq 24 \log(2N)$, whereas that for SRS-SC is $n = \Omega(\{\log(N)\}^2)$. More importantly, the misclustered rate of DCS-SC has the same convergence rate as that of SRS-SC. This demonstrates that DCS-SC can be more effective than SRS-SC.

5. Numerical studies. In this section, we present three simulation scenarios to examine the performances of both DCS-SC and SRS-SC.

5.1. Simulation models and performance measurements. In the simulation studies, we use the SBM model to generate networks with $K = 3$ communities. The block matrix B is controlled by two parameters β and ζ and is constructed as follows:

$$(6) \quad B = \beta\{(1 - \zeta) * I_K + \zeta \mathbf{1}_K \mathbf{1}_K^\top\},$$

where $\beta \in [0, 1]$ is the connection intensity, $\zeta \in [0, 1]$ is the connection out-in-ratio, $I_K \in \mathbb{R}^{K \times K}$ is an identity matrix, and $\mathbf{1}_K \in \mathbb{R}^K$ is filled with elements 1. Additionally, the community labels of the nodes are generated from an independent multinomial distribution with $\pi \in \mathbb{R}^K$.

SCENARIO 1 (Consistency of SSC) We set $\beta = 0.1$, $\zeta = 0.05$ and $\pi = (1/3, 1/3, 1/3)^\top$. Then, to demonstrate the consistency of the SSC algorithm, we let the size of network N grow from 5,000 to 30,000. Moreover, based on Theorems 4.5 and 4.7, for each setting of N , we set n to be $\lceil 2\{\log(N)\}^2 \rceil$, where $\lceil x \rceil$ is the smallest integer greater than or equal to a real number x .

SCENARIO 2 (Effect of subsample size on SSC) We set $N = 12,000$, $\beta = 0.03$, $\zeta = 0.05$, and $\pi = (1/3, 1/3, 1/3)^\top$. To reflect the effect of the subsample size, n is set to vary from 100 to 1,100.

SCENARIO 3 (Effect of signal strength on SSC) According to the SBM block matrix defined in (6), the signal strength of community membership depends on β and ζ . Here, we fix $N = 12,000$ and $n = 100$ and set the multinomial distribution as $\pi = (1/3, 1/3, 1/3)^\top$. Then, to examine the effect of β and ζ , we set β to increase from 0 to 0.95. Correspondingly, ζ increases from 0 to 0.95.

SCENARIO 4 (Effect of imbalance on SSC) Under this scenario, we fix the network size $N = 12,000$, $n = 100$, $\beta = 0.1$, and $\zeta = 0.05$. To reflect the imbalance of the network cluster, we set $\pi = (1/3 - \Delta, 1/3, 1/3 + \Delta)^\top$ with Δ varying from 0 to 0.3, where a larger Δ implies greater imbalance in the cluster size.

To evaluate clustering performance, we consider the misclustered rate, which has been widely used in the investigation of community detection under SBM (Gao et al., 2018). Let $\hat{Z} \in \mathbb{R}^{N \times K}$ be the estimated membership matrix. Then, the misclustered rate is calculated as

$$(7) \quad \mathcal{R}(\hat{Z}, Z) = \frac{1}{N} \min_{\theta \in \mathbb{E}_K} d(\hat{Z}\theta, Z),$$

where \mathbb{E}_K is the set of all $K \times K$ permutation matrices, and $d(\cdot, \cdot)$ is the distance function of two matrices with the same dimension. It counts the number of different rows between these two matrices (i.e., $d(\hat{Z}, Z) = \sum_{i=1}^N I(\hat{Z}_i \neq Z_i)$). For a reliable evaluation, the random experiments are repeated $T = 100$ times. All simulations are conducted in Python using a Dell computer with a 3.70 GHz Intel Core i9 processor.

5.2. Simulation results. The detailed results are presented in Figures 10–13. We can draw the following conclusions based on the simulation results.

SCENARIO 1. The result of Scenario 1 is shown in Figure 10. We draw the following conclusions. First, as N increases, the misclustered rates of both SRS-SC and DCS-SC decrease, becoming close to 0. Moreover, Figure 10 shows that the standard errors of these two algorithms also decrease as N grows. Second, as we can observe from the right panel of Figure 10, as the network size increases, the computational time of SC increases drastically compared with SRS-SC and DCS-SC. These results not only support the theoretical conclusions of Theorems 4.5 and 4.7 but also justify our motivation and intuition to conduct SSC.

SCENARIO 2. Figure 11 indicates the effect of n on the performance of SRS-SC and DCS-SC. First, as subsample size n grows, the misclustered rates of these two algorithms decrease. Second, as shown in Figure 11, when $n = 300$, the misclustered rates of SRS-SC and DCS-SC are both below 0.100, but the average computational time of these two algorithms is no greater than 2.000s. As a result, both SRS-SC and DCS-SC could be applied in large-scale networks for community detection. This corroborates the theoretical findings in Theorems 4.5 and 4.7.

SCENARIO 3. Figure 12 and Table 2 show the performance of the methods when the signal strength varies. First, as presented in Table 2, the performances of these two methods are

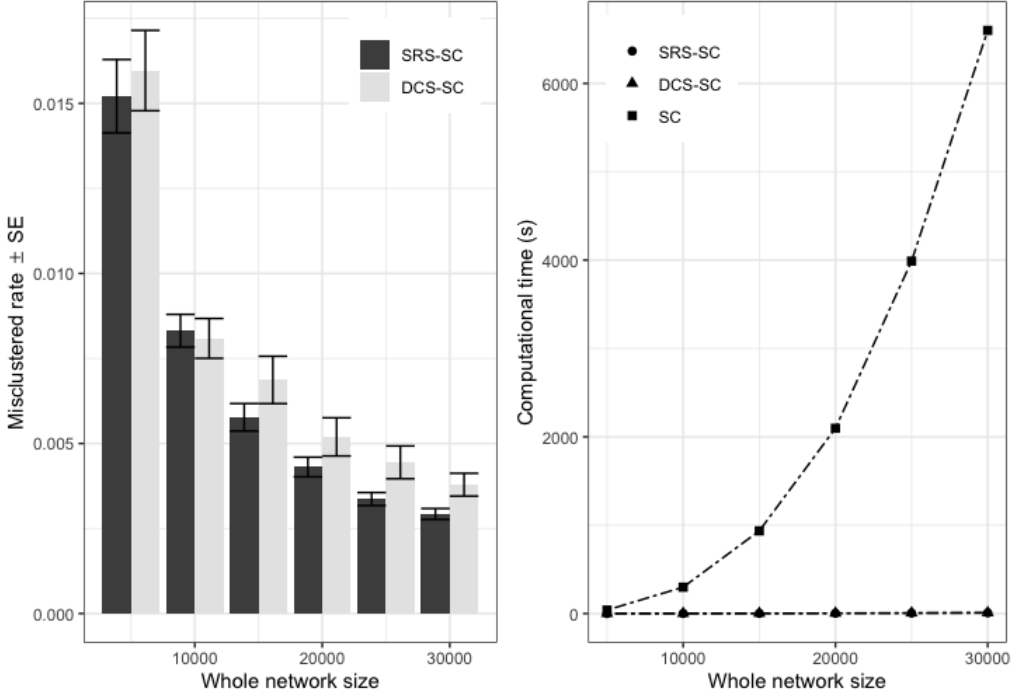


FIG 10. The misclustered rate (left panel) N grows from 5,000 to 30,000. Here, the subsample size is $n = \lceil 2\{\log(N)\}^2 \rceil$. Further, the standard error (SE) is reported by the error bar in the left panel. The average computational times (right panel) of the SRS-SC, DCS-SC, and spectral clustering (SC) algorithm are further compared as N increases.

TABLE 2

Simulation results of SRS-SC and DCS-SC with β and ζ varying from 0.05 to 0.95. The misclustered rates of the SRS-SC and DCS-SC are reported accordingly. In addition, the standard error of the misclustered rate is reported between parentheses.

| $\beta \setminus \zeta$ | | 0.05 | 0.35 | 0.65 | 0.95 |
|-------------------------|--------|------------|------------|------------|------------|
| 0.05 | SRS-SC | .173(.005) | .421(.042) | .620(.008) | .661(.001) |
| | DCS-SC | .169(.004) | .347(.002) | .610(.007) | .661(.001) |
| 0.35 | SRS-SC | .000(.000) | .024(.001) | .286(.038) | .656(.002) |
| | DCS-SC | .000(.000) | .025(.001) | .220(.002) | .657(.001) |
| 0.65 | SRS-SC | .000(.000) | .000(.000) | .060(.003) | .647(.003) |
| | DCS-SC | .000(.000) | .001(.000) | .057(.001) | .646(.002) |
| 0.95 | SRS-SC | .000(.000) | .000(.000) | .000(.000) | .541(.011) |
| | DCS-SC | .000(.000) | .000(.000) | .001(.000) | .546(.003) |

satisfactory, except that the connection strength β is extremely small or the connection out-in-ratio ζ is very large. This means that, faced with fuzzy community structures and sparse scenarios, the subsample size needs to be increased appropriately for more accurate community detection. Second, for $\beta = 0.95$, as ζ decreases from 0.95 to 0.05, the misclustered rates of SRS-SC and DCS-SC both drop to 0.000. Moreover, for $\zeta = 0.05$, as β varies from 0.05 to 0.95, the misclustered rates of these two methods decrease to 0.000. The results verify the theoretical conclusions of Theorems 4.5 and 4.7. Namely, the misclustered rate decreases as the signal strength increases. This phenomenon is also confirmed by Figure 12.

SCENARIO 4. Figure 13 shows that different imbalance levels have different effects on the performance of SRS-SC and DCS-SC. First, as Δ increases from 0 to 0.1, the misclustered

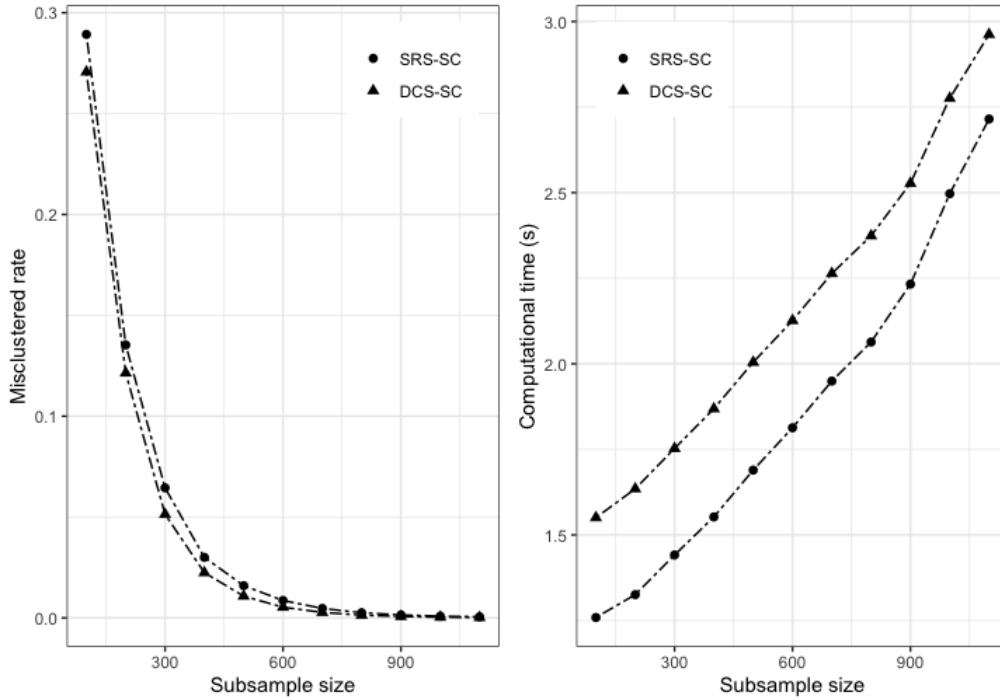


FIG 11. The effect of subsample size n on the performance of SRS-SC and DCS-SC. Subsample size n varies from 100 to 1,100. Left panel: relationship between the misclustered rate and subsample size n . Right panel: computational time versus subsample size n .

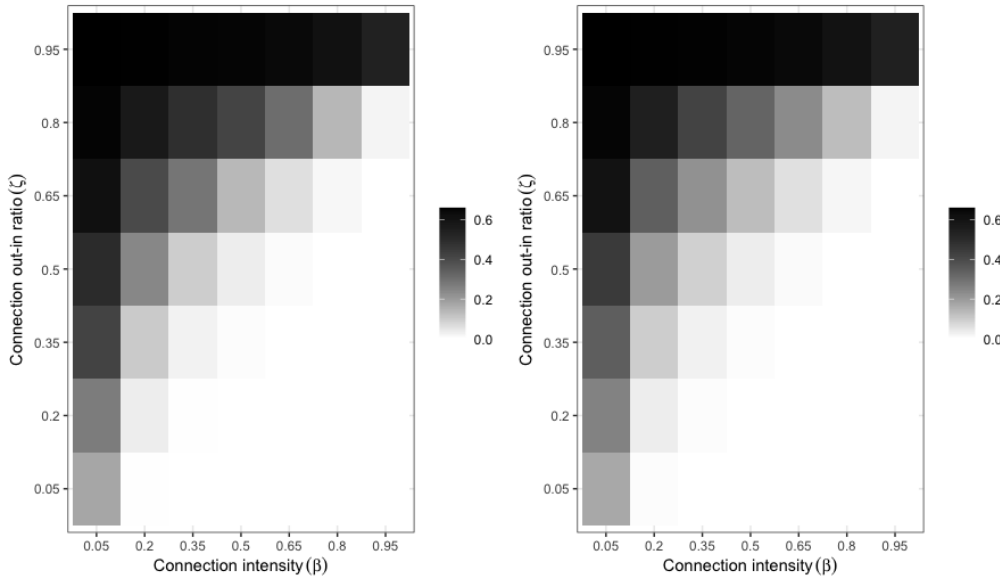


FIG 12. The effect of β and ζ under SRS-SC (left panel) and DCS-SC (right panel). The average misclustered rate is represented by the gray scale. Evidently, a stronger connection intensity and smaller connection out-in-ratio yield more accurate clustering results for these two methods.

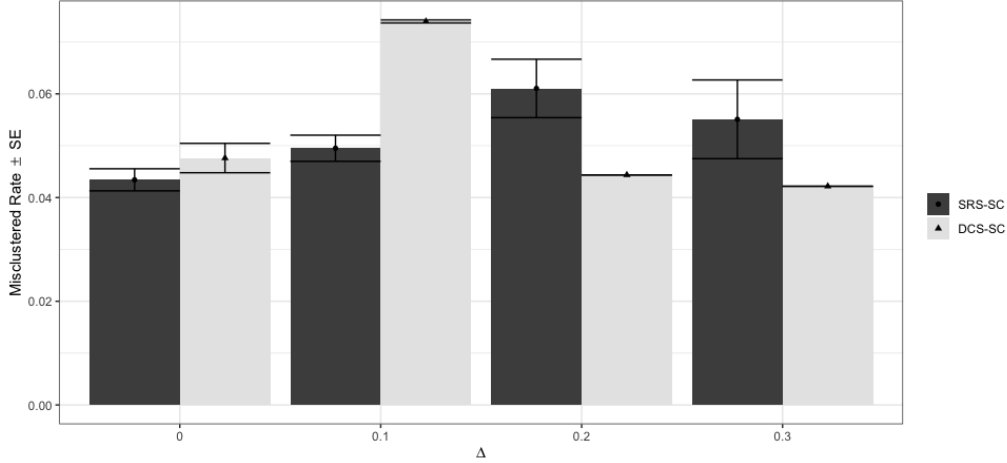


FIG 13. Simulation results of SRS-SC and DCS-SC for the subsample size of Δ varying from 0 to 0.3. The misclustered rates of SRS-SC and DCS-SC are reported accordingly. In addition, the standard error (SE) is reported by the error bar.

rates of these two methods increase. As Δ increases slightly, it is difficult to cover all communities with a small subsample size. Second, as Δ increases from 0.1 to 0.3, the misclustered rate of the DCS-SC declines. However, the misclustered rate of SRS-SC increases initially and then decreases. Because the difference in the degree of nodes between communities becomes larger, DCS can collect more informative subsamples. Moreover, the community structure is more clearly represented by the bi-adjacency matrix. Finally, the standard error of DCS-SC drops to 0.000 as Δ increases. Therefore, for high imbalance cases, DCS-SC obtains more stable and accurate clustering results.

Based on the empirical performance of SSC on these simulation studies, our proposed method is efficient and robust for analyzing large-scale networks. Additionally, the DCS method is more recommended for selecting a small node set from the entire network.

6. Discussion. In this study, we present an SSC algorithm to identify the community structure of large social networks. Particularly, we discuss two subsampling methods (i.e., SRS and DCS). Theoretically, we investigate the subsample sizes for these two methods and establish the statistical properties of the clustering results. The computational complexity of the SSC algorithm can be reduced to $O(Nn^2)$, where n is the subsample size, which can be as low as $\Omega\{\log(N)^2\}$. The empirical results illustrate that we could identify 88.2% of the user community tags with only 0.2% of the time of the spectral clustering result based on the whole network. This result can help the Sina Weibo platform to understand the user's market profile in market research effectively.

The idea of the paper can be extended to research on other network data with more complex relationships, such as bipartite and multiple networks, which we are currently investigating. Additionally, here we study the subsampling method, which only needs to select the node set once. Another interesting issue in future research is to develop a multi-step subsampling method which can extract richer network structure information.

Funding. Danyang Huang is supported by the National Natural Science Foundation of China (NSFC, 12071477), building world-class universities (disciplines) of the Renmin University of China. Bo Zhang is supported by the National Natural Science Foundation of China (NSFC, 71873137), building world-class universities (disciplines) of the Renmin University of China.

REFERENCES

- Awasthi, P. and Sheffet, O. (2012), “Improved spectral-norm bounds for clustering,” in *Approximation, Randomization, and Combinatorial Optimization. Algorithms and Techniques*, Springer, pp. 37–49.
- Binkiewicz, N., Vogelstein, J. T., and Rohe, K. (2017), “Covariate-assisted spectral clustering,” *Biometrika*, 104, 361–377.
- Chen, W.-Y., Song, Y., Bai, H., Lin, C.-J., and Chang, E. Y. (2010), “Parallel spectral clustering in distributed systems,” *IEEE Transactions on Pattern Analysis and Machine Intelligence*, 33, 568–586.
- Chen, X. and Cai, D. (2011), “Large scale spectral clustering with landmark-based representation,” in *Proceedings of the AAAI Conference on Artificial Intelligence*, vol. 25.
- Drineas, P. and Mahoney, M. W. (2005), “On the Nyström method for approximating a Gram matrix for improved kernel-based learning,” *The Journal of Machine Learning Research*, 6, 2153–2175.
- Fortunato, S. (2010), “Community detection in graphs,” *Physics Reports*, 486, 75–174.
- Fowlkes, C., Belongie, S., Chung, F., and Malik, J. (2004), “Spectral grouping using the Nyström method,” *IEEE Transactions on Pattern Analysis and Machine Intelligence*, 26, 214–225.
- Gao, C., Ma, Z., Zhang, A. Y., Zhou, H. H., et al. (2018), “Community detection in degree-corrected block models,” *The Annals of Statistics*, 46, 2153–2185.
- Girvan, M. and Newman, M. E. (2002), “Community structure in social and biological networks,” *Proceedings of the National Academy of Sciences*, 99, 7821–7826.
- Harenberg, S., Bello, G., Gjeltema, L., Ranshous, S., Harlalka, J., Seay, R., Padmanabhan, K., and Samatova, N. (2014), “Community detection in large-scale networks: a survey and empirical evaluation,” *Wiley Interdisciplinary Reviews: Computational Statistics*, 6, 426–439.
- Holland, P. W., Laskey, K. B., and Leinhardt, S. (1983), “Stochastic blockmodels: First steps,” *Social Networks*, 5, 109–137.
- Homburg, C. (2021), “Wage Inequality: Its Impact on Customer Satisfaction and Firm Performance,” *Journal of Marketing*.
- Joseph, A., Yu, B., et al. (2016), “Impact of regularization on spectral clustering,” *The Annals of Statistics*, 44, 1765–1791.
- Knuth, D. E. (1976), “Big omicron and big omega and big theta,” *ACM Sigact News*, 8, 18–24.
- Krzakala, F., Moore, C., Mossel, E., Neeman, J., Sly, A., Zdeborová, L., and Zhang, P. (2013), “Spectral redemption in clustering sparse networks,” *Proceedings of the National Academy of Sciences*, 110, 20935–20940.
- Lancichinetti, A. and Fortunato, S. (2009), “Community detection algorithms: a comparative analysis,” *Physical Review E*, 80, 056117.
- Lei, J., Rinaldo, A., et al. (2015), “Consistency of spectral clustering in stochastic block models,” *The Annals of Statistics*, 43, 215–237.
- Li, M., Lian, X.-C., Kwok, J. T., and Lu, B.-L. (2011), “Time and space efficient spectral clustering via column sampling,” in *CVPR 2011*, IEEE, pp. 2297–2304.
- Newman, M. E. and Girvan, M. (2004), “Finding and evaluating community structure in networks,” *Physical Review E*, 69, 026113.
- Ng, A. Y., Jordan, M. I., and Weiss, Y. (2002), “On spectral clustering: Analysis and an algorithm,” in *Advances in Neural Information Processing Systems*, pp. 849–856.
- Rohe, K., Chatterjee, S., Yu, B., et al. (2011), “Spectral clustering and the high-dimensional stochastic block-model,” *The Annals of Statistics*, 39, 1878–1915.
- Shaddy, F. and Shah, A. K. (2021), “EXPRESS: When to Use Markets, Lines, and Lotteries: How Beliefs About Preferences Shape Beliefs About Allocation,” *Journal of Marketing*, 00222429211012107.
- Vitter, J. S. (1985), “Random sampling with a reservoir,” *ACM Transactions on Mathematical Software (TOMS)*, 11, 37–57.
- Von Luxburg, U. (2007), “A tutorial on spectral clustering,” *Statistics and Computing*, 17, 395–416.
- Wang, H., Yang, M., and Stufken, J. (2019), “Information-based optimal subdata selection for big data linear regression,” *Journal of the American Statistical Association*, 114, 393–405.
- Wang, H., Zhu, R., and Ma, P. (2018), “Optimal subsampling for large sample logistic regression,” *Journal of the American Statistical Association*, 113, 829–844.
- Yan, D., Huang, L., and Jordan, M. I. (2009), “Fast approximate spectral clustering,” in *Proceedings of the 15th ACM SIGKDD International Conference on Knowledge Discovery and Data Mining*, pp. 907–916.
- Yang, Y., Zhang, K., and Kannan, P. (2021), “EXPRESS: Identifying Market Structure: A Deep Network Representation Learning of Social Engagement,” *Journal of Marketing*, 00222429211033585.